# scientific reports



### **OPEN**

# Pembrolizumab promotes degradation of cyclin dependent kinase 6 and suppresses ovarian cancer progression in vitro

Yi Wu<sup>1⊠</sup>, Ziyan Xu², Zuqiang Kou³, Qiuling Ye⁴, Liting Chen⁴ & Boyu Gou⁴

Pembrolizumab is a novel humanized anti-PD-1 monoclonal antibody capable of enhancing T-cell mediated antitumor immunity. However, the function of pembrolizumab on tumor cells themselves and relative molecular mechanism in ovarian cancer remain unknown. Our study demonstrated pembrolizumab exerted remarkable suppressive impacts on proliferation, colony formation and migration of ovarian cancer cells in vitro. Furthermore, pembrolizumab treatment delayed cell cycle progress from G1 to S phase transition and suppressed cell growth in ovarian cancer cells. Mechanistically, pembrolizumab decreased the stability of CDK6 protein through a polyubiquitin-mediated proteasomal degradation pathway. Meanwhile, pembrolizumab treatment dose-dependently reduced Snail, Vimentin and N-cadherin expressions and enhanced E-cadherin expressions. Additionally, the combined treatment of pembrolizumab and cisplatin effectively enhanced anti-proliferative effect of cisplatin on HO-8910 cells. These findings suggested pembrolizumab efficiently suppressed malignant progression of ovarian cancer cells and facilitated proteasomal degradation of CDK6 and increased cisplatin inhibition of HO-8910 cells proliferation, therefore providing a promising therapeutic strategy for ovarian cancer.

Keywords Pembrolizumab, Ovarian cancer, CDK6, Cisplatin

#### Abbreviations

OC Ovarian cancer

CDK6 Cyclin-dependent kinase 6 CDK4 Cyclin-dependent kinase 4

CCND1 Cyclin D1

mTOR Mechanistic target of rapamycin kinase

PFS Progression-free survival PD-1 Programmed cell death protein 1

CCK-8 The cell counting kit-8

UBE2N Ubiquitin-conjugating enzyme 2N VEGFA Vascular endothelial growth factor A FLT3 Fms-related tyrosine kinase 3 EMT Epithelial-to-mesenchymal transition

AURK Aurora kinase CHX Cycloheximide

Ovarian cancer (OC) is one of the most common gynecological cancers. In 2022, ovarian cancer is the 8th leading cause of global female cancer incidence, with comprising 3.4% of female cancer cases and the eighth leading cause of female cancer mortality worldwide, with 4.8% of female cancer deaths<sup>1</sup>. Because of hidden onset and rapid progression, more than one-half of ovarian cancer patients are diagnosed as late stage<sup>2</sup>. The five-year survival rate for ovarian cancer patients is no more than 30%<sup>3</sup>. The current standard treatment for ovarian cancer

<sup>1</sup>Department of Pathogenic Biology, Shenyang Medical College, Shenyang, Liaoning 110004, People's Republic of China. <sup>2</sup>Major in Anesthesiology, Shenyang Medical College, Shenyang, Liaoning 110004, People's Republic of China. <sup>3</sup>Department of Logistics, Shenyang Ligong University, Shenyang, Liaoning 110004, People's Republic of China. <sup>4</sup>Major in Medical Laboratory Technology, School of Basic Medicine, Shenyang Medical College, Shenyang, Liaoning 110004, People's Republic of China. <sup>2</sup>email: wuyi@symc.edu.cn

consists of cytoreductive surgery followed by platinum-based chemotherapy<sup>4</sup>. Cisplatin, as a platinum compound agent and the first-line therapeutic drug for ovarian cancer treatment, has shown remarkable efficacy. However, about 75% of ovarian cancer patients have developed cisplatin resistance or even multiple drug resistance after years of treatment, leading to treatment failure<sup>5</sup>. Therefore, it is of particular urgency to uncover and identify novel drugs and pharmacological targets for improving treatment efficacy of ovarian cancer.

Pembrolizumab is an anti-PD-1 highly selective, humanized monoclonal IgG4-kappa isotype antibody capable of blocking PD-1 receptor by binding to the PD-1 receptor, leading to a physiological shift to immune reactivity and anti-tumor effect, so as to restore the anti-tumor immune response of T cells to play an anti-tumor role<sup>6,7</sup>. Clinically, PD-1 blockade elicits potent antitumor immune responses, and antibodies blocking PD-1 ligation, including pembrolizumab, have recently received Food and Drug Administration approval for the treatment of advanced melanoma, renal cell cancer, and non-small cell lung cancer, and with a clinical trial in ovarian cancer as well<sup>8,9</sup>. In recent years, although it is well known that pembrolizumab has widely been used for immunotherapy for cancer based on T cells, whether pembrolizumab can directly target tumor cells themselves remain to be elusive.

Cyclin-dependent kinase 6 (CDK6) is an important regulator of the cell cycle<sup>10</sup>. It is the catalytic subunit of the CDK6-cyclin D complex involved in the G1 to S cell cycle progression and negatively regulates cell differentiation<sup>11</sup>. Emerging evidence suggests that certain tumor cells require CDK6 for proliferation<sup>11</sup>. CDK6 is frequently overexpressed or hyper-activated in cancer samples<sup>12</sup>. Recent studies showed that CDK6 was significantly upregulated in ovarian cancer tissues and positively correlated with ovarian cancer progression<sup>13</sup>. Moreover, high CDK6 expression was significantly associated with early relapse and predicted a shorter progression-free survival (PFS) of OC patients, implying a specific oncogenic role of CDK6 in OC<sup>14</sup>.

In this study, we provided evidence that pembrolizumab, as anti-PD-1 drug, significantly promotes CDK6 ubiquitination and degradation, accompanied by inducing G0/G1 cell cycle arrest, reducing cell proliferation and migration, and enhancing the anti-proliferative efficacy of cisplatin in OC cells. Overall, our findings unveil a previously unexplored role for pembrolizumab in suppressing ovarian cancer progression and accelerating CDK6 degradation.

#### Materials and methods Reagents

Reagents used in this study included pembrolizumab (MedChemExpress, MCE), cisplatin (MedChemExpress, MCE), cycloheximide (CHX) (MedChemExpress, MCE) and MG132 (Cell Signaling Technology, CST).

#### Cell lines and cell culture

HO-8910 and CAOV-3 cell lines were purchased from the American Type Culture Collection (ATCC). Human ovarian cancer HO-8910 cells were cultured in RPMI-1640 (Gibco) medium supplemented with 10% fetal bovine serum (FBS) (BI), penicillin (100 U/mL) and streptomycin (100  $\mu$ g/mL). Human ovarian cancer CAOV-3 cells were cultured in DMEM (Gibco) medium supplemented with 10% fetal bovine serum (FBS) (BI), penicillin (100 U/mL) and) streptomycin (100  $\mu$ g/mL). Cells were incubated with 5% CO, at 37 °C.

#### CCK-8 assays

CCK-8 assay was used to evaluate cell viability. Human ovarian cancer HO-8910 or CAOV-3 cells were planted on 96-well plates at 3000 cells per well. After incubation for 24 h, cells were treated with a range of concentrations of pembrolizumab for 72 h. Additionally, cells were exposed to 20  $\mu$ g/mL pembrolizumab and incubated for 24 h, 48 h and 72 h. Then, the cell Counting kit-8 (CCK-8, Bimake, USA) was used to detect cell proliferation. Generally, 10  $\mu$ L CCK-8 solutions was added to each plate and cells were incubated at 37 °C for 1 h. Cell viability was determined by absorbance at 450 nm. Each treatment was performed in triplicate, and data are shown as mean  $\pm$  SEM.

#### Clone formation assay

HO-8910 and CAOV-3 cells were planted in 6-well plates at 1000 cells per well and incubated for 24 h, and then treated with different concentrations of pembrolizumab. After cultured at 37 °C 5% CO $_2$  incubator for one week, the clones were fixed with 4% paraformaldehyde and stained with crystal violet (0.1%, m/v). The cell clones were counted with the Image J software.

#### Migration assays

The two-dimensional migration ability of HO-8910 and CAOV-3 cells was detected by wound-healing assays and Transwell migration assay. For wound-healing assays, cells were seeded in six-well plates and cultured to monolayer confluency in normal medium. A wound was made by dragging a sterile 10  $\mu$ L pipette tip across the well and the detached cells were removed by three phosphate buffer saline (PBS) washes. The remaining cells were cultured at 37 °C with or without pembrolizumab treatment in serum-free RPMI-1640 medium or serum-free DMEM medium. Migrating cells at the wound front were photographed at 0 h, 24 h, 48 h and 72 h.

For Transwell migration assay, cell migration assays were performed using 24-well Transwell chambers with polycarbonate filter inserts (8  $\mu m$  pore size, Corning Costar) uncoated with Matrigel. About  $3\times10^4$  cells were suspended in 100  $\mu L$  serum-free RPMI-1640 medium with pembrolizumab or vehicle and added to the upper chamber, while 600  $\mu L$  RPMI-1640 medium or DMEM medium containing 10% FBS and pembrolizumab or vehicle was placed in the lower chamber. After 15 h of incubation, the cells remaining in the upper chamber were removed using cotton swabs. The cells that migrated through the membrane and adhered to the lower surface of the membrane were fixed with 95% ethanol and stained with 0.1% crystal violet. Cells in 5 microscopic fields were photographed and counted with Image J 1.49V software.

#### RNA isolation and quantitative real-time PCR (gRT-PCR)

HO-8910 and CAOV-3 ovarian cancer cells were pre-treated with 20 µg/mL pembrolizumab or vehicle for 24 h. The total RNA from HO-8910 and CAOV-3 cells was isolated using Trizol Reagent (Invitrogen) according to the manufacturer's instructions. The PrimeScript™ RT-PCR Kit (TaKaRa) was used to transcribe RNA to cDNA. cDNA was used for subsequent qRT-PCR using the SYBR Premix Ex Taq kit (TaKaRa). Each reaction was run on the Light Cycler 96 Realtime PCR machine (Roche Life Science). Messenger RNA expression levels were normalized to ribosome 18 s rRNA. The sequences of the primers were listed in Supplementary Table 1.

#### Western blotting analysis

Cells were lysed in a RIPA lysis buffer which was added with protease inhibitors (APExBIO). Protein from cell lysates ( $10\,\mu g$  0f. total protein) were fractionated by SDS-PAGE and transferred to PVDF membranes (Millipore, USA) using a wet transfer system. After blocking in 5% non-fat milk at room temperature for 1 h, the membranes were incubated with corresponding primary antibodies at an appropriate dilution overnight at 4 °C. Membranes were further probed with horseradish peroxidase-conjugated secondary antibodies for 1 h at room temperature. The immunoreactive bands were visualized by enhanced chemiluminescence (ECL) detection system (Tanon, Shanghai, China). The following primary antibodies were purchased: anti-CDK6 (1:1000, #13331 T, R; 1:1000, #3136 T, M, Cell Signaling Technology), anti-Vimentin (1:1000, #5741 T, Cell Signaling Technology), anti-E-Cadherin (1:1000, #3195 T, Cell Signaling Technology), anti-Snail (1:1000, #3879P, Cell Signaling Technology), anti-N-Cadherin (1:2000, #62219–1-lg, Proteintech), anti-ubiquitin (1:500, #10201–2-AP, Proteintech), PD-1 (1:1000, #18106–1-AP) and anti-GAPDH (1:20,000, #60004–1-lg, Proteintech). Additionally, all the blots were cut prior to hybridisation with antibodies during blotting.

#### Immunoprecipitation assay

Cells were lysed in IP buffer with a protease inhibitor cocktail (Roche) for 30 min on the ice and centrifuged at 12,000 g for 20 min at 4 °C. The supernatant was obtained. Equal amounts of lysate were incubated with the appropriate primary antibodies and protein A/G agarose beads (GE Healthcare) overnight at 4 °C. The beads were washed three times with lysis buffer and then prepared for western blotting. Both immunoprecipitates and lysates were examined by the corresponding primary antibodies.

#### Statistical analysis

Statistical analyses were executed by using the Graphpad 5.0 software. The experimental values were presented as mean  $\pm$  standard error of the mean (SEM). Unpaired Student's t test was used to compare means in two independent samples. Statistically significant differences of multiple groups were determined by one-way analysis of variance (ANOVA) followed by Tukey's test. When P-values were less than 0.05, statistical significance was assumed.

#### Results

#### Pembrolizumab inhibits OC cell growth and proliferation

Considering that Pembrolizumab is a targeting PD-1 monoclonal antibody, we detected the expression of intrinsic PD-1 on HO-8910 and CAOV-3 cells. Immunoblot analysis revealed that PD-1 was expressed by HO-8910 and CAOV-3 cells (Supplementary Fig. 1).

To assess whether pembrolizumab, an immune checkpoint inhibitor, has the direct anti-proliferative influence on ovarian cancer cells, CCK-8 assay was first performed in OC cells. HO-8910 and CAOV-3 cells were treated with a range of pembrolizumab concentration (0, 0.5, 1.0, 2.0, 5.0, 10, 20  $\mu$ g/mL) for 72 h or 20  $\mu$ g/mL of pembrolizumab for 24 h, 48 h and 72 h. IC50 of HO-8910 and CAOV-3 cells to pembrolizumab was 21.07  $\mu$ g/mL and 15.52  $\mu$ g/mL respectively. As shown in Fig. 1A-D, the viabilities of both OC cell lines were significantly suppressed in a dose-dependent as well as time-dependent manner. In order to test the long-term influence of pembrolizumab treatment on cancer cells, we then performed colony formation experiments. Our results showed pembrolizumab treatment significantly decreased cell colony formation in HO-8910 or CAOV-3 cells in a dose-dependent manner after one week of cultures. Pembrolizumab treatment decreased HO-8901 cell colony numbers by 13.3%, 55.1% and 90.5%, respectively; CAOV-3 cells colony numbers by 26.9%, 55.4% and 64.3%, respectively (Fig. 1E-F, Supplementary Fig. 9). In summary, these findings indicated that pembrolizumab exhibits directly inhibitory influence on growth and proliferation of ovarian cancer cells.

#### Pembrolizumab treatment causes G0/G1 arrest in ovarian cancer cells

To identify whether pembrolizumab inhibited OC cell growth and proliferation through induction of cell cycle arrest, a flow cytometric analysis was performed in HO-8910 and CAOV-3 cells stained with propidium iodine. We monitored the cell cycle progression of each group of OC cells exposed to pembrolizumab or vehicle. We found that pembrolizumab treatment in HO-8910 cells markedly induced G0/G1 cell cycle arrest after 48 h, which was associated with the decreased population in S phases from 34.9% to 26.84% and the increased population in G1 phases from 58.58% to 64.63% (Fig. 2A-B). We next tested whether pembrolizumab plays the similar part in CAOV-3 cells. As expected, the results from CAOV-3 cells suggested that the number of cells in G1 increased from 46.6% to 52.72%, and S phase decreased from 30.19% to 21.96% (Fig. 2A-B). Collectively, these results indicated that pembrolizumab suppresses the growth and proliferation of OC cells, possibly via delaying cell G1-S phase transition.

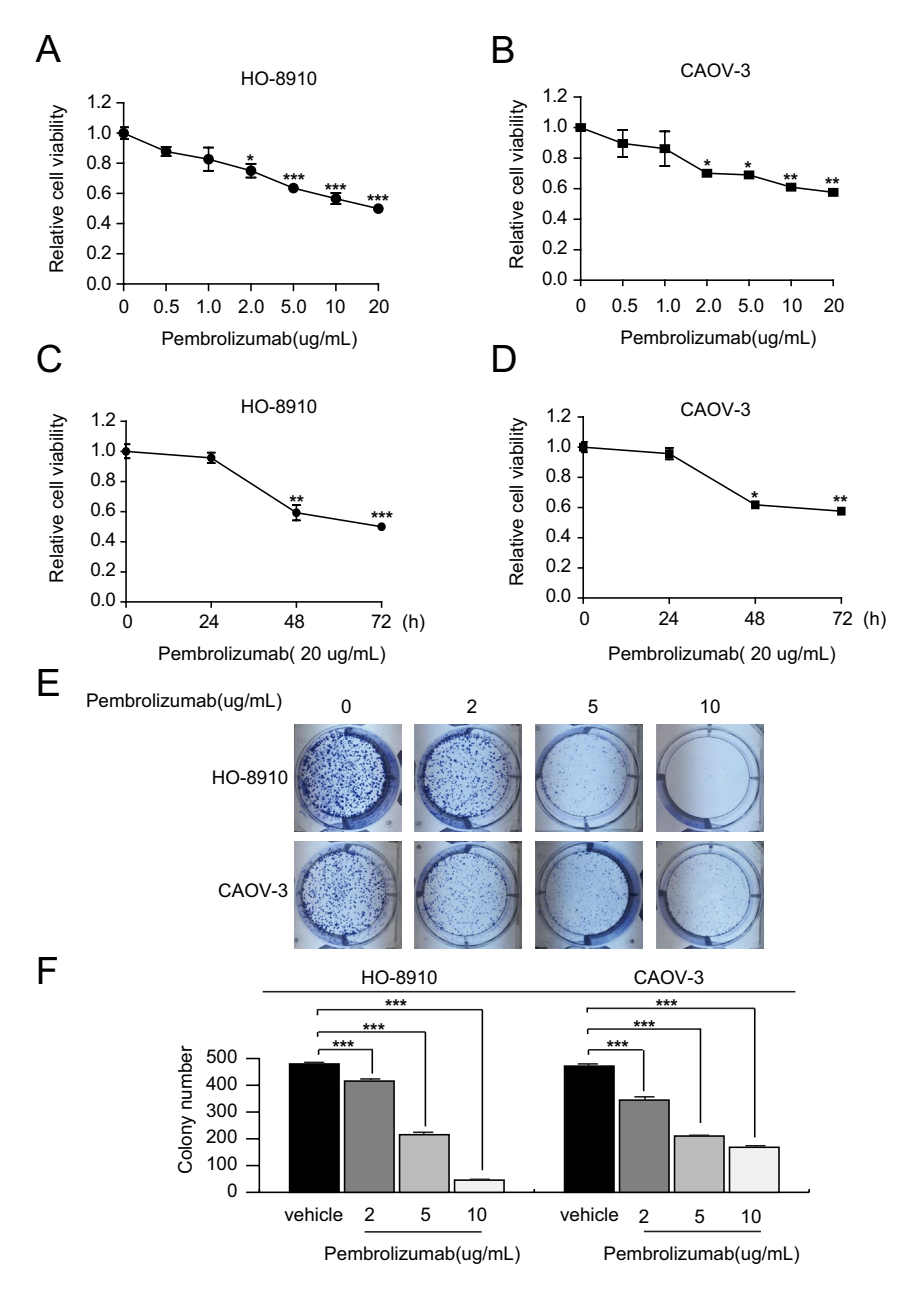


**Fig. 1.** Effect of pembrolizumab on HO-8910 and CAOV-3 cells proliferation. (**A-B**) HO-8910 and CAOV-3 cells were exposed to pembrolizumab (0, 0.5, 1.0, 2.0, 5.0, 10, 20 μg/mL) for 72 h. And then CCK-8 assays were performed to determine the cell viability. The data are expressed as mean ± SEM. \*P<0.05; \*\*P<0.01; \*\*\* P<0.001 compared with Control group (0 μg/mL pembrolizumab). (**C-D**) HO-8910 and CAOV-3 cells were exposed to pembrolizumab (20 μg/mL) for 24 h, 48 h and 72 h. And then CCK-8 assays were performed to determine the cell viability. The data are expressed as mean ± SEM. \*P<0.05; \*\*P<0.01; \*\*\* P<0.001 compared with Control group (0 h). (**E**) Long-term colony formation assays of HO-8910 and CAOV-3 cells treated with pembrolizumab (0, 2.0, 5.0, 10μg/mL) for one week. (**F**) Colony numbers of HO-8910 and CAOV-3 cells were counted using Image J software. The data are expressed as mean ± SEM. \*\*\*P<0.001 compared with Control group (0 μg/mL pembrolizumab).

## Pembrolizumab promotes CDK6 ubiquitination and its subsequent degradation in HO-8910 cells

To dissect the possible molecular mechanisms by which pembrolizumab regulates cell cycle progression in OC cells, we performed Western blotting to examine the influence of pembrolizumab on the expression of cell cycle-related protein, which is involved in the regulation of G1 to S phase transition of the cell cycle. After the exposure of HO-8910 cells to gradient concentrations of pembrolizumab for 48 h, the protein levels of CCND1, CDK4 and CDK6 were assessed. The results demonstrated that CDK6 expression in pembrolizumab-treated HO-8910 cells dramatically decreased in a dose-dependent manner without significantly affecting the protein levels of CCND1 and CDK4. (Fig. 3A-B left panel; Supplementary Fig. 2; Supplementary Fig. 3). Consistently, the levels of CDK6

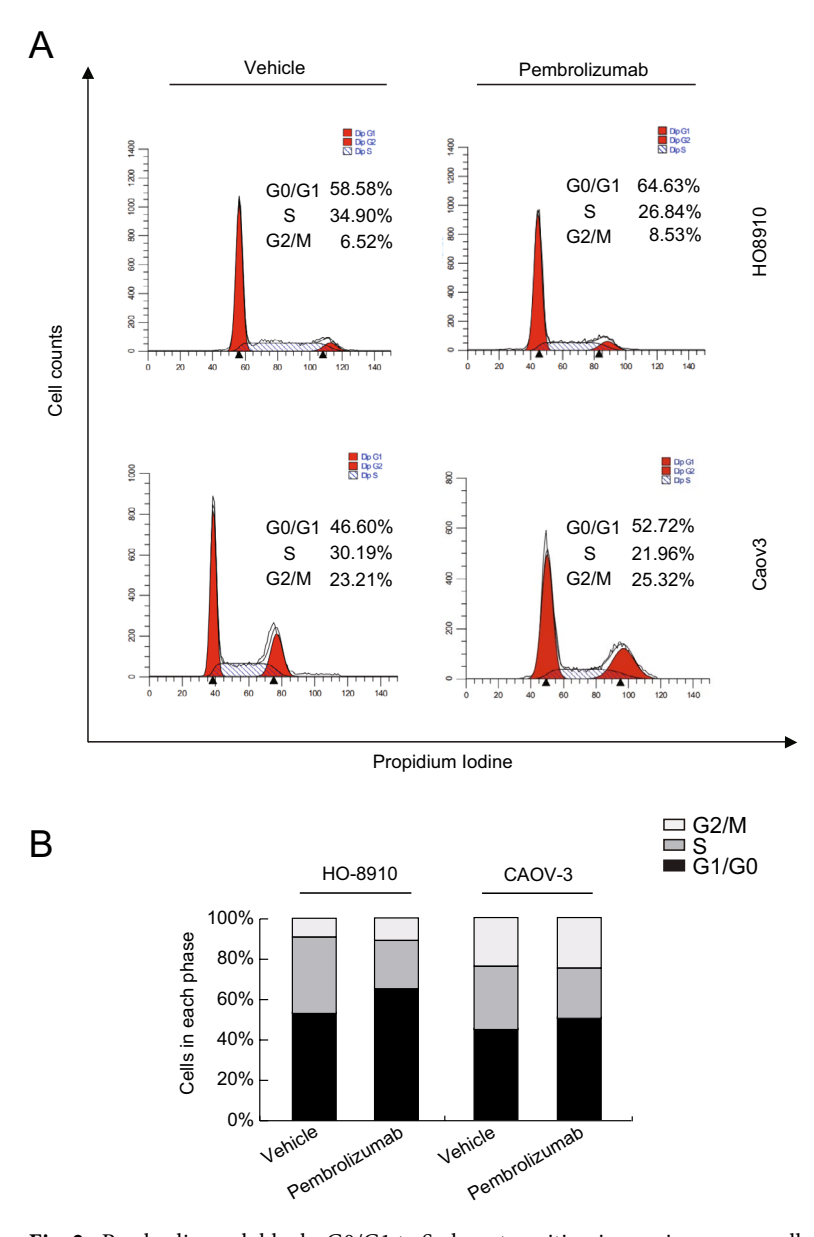
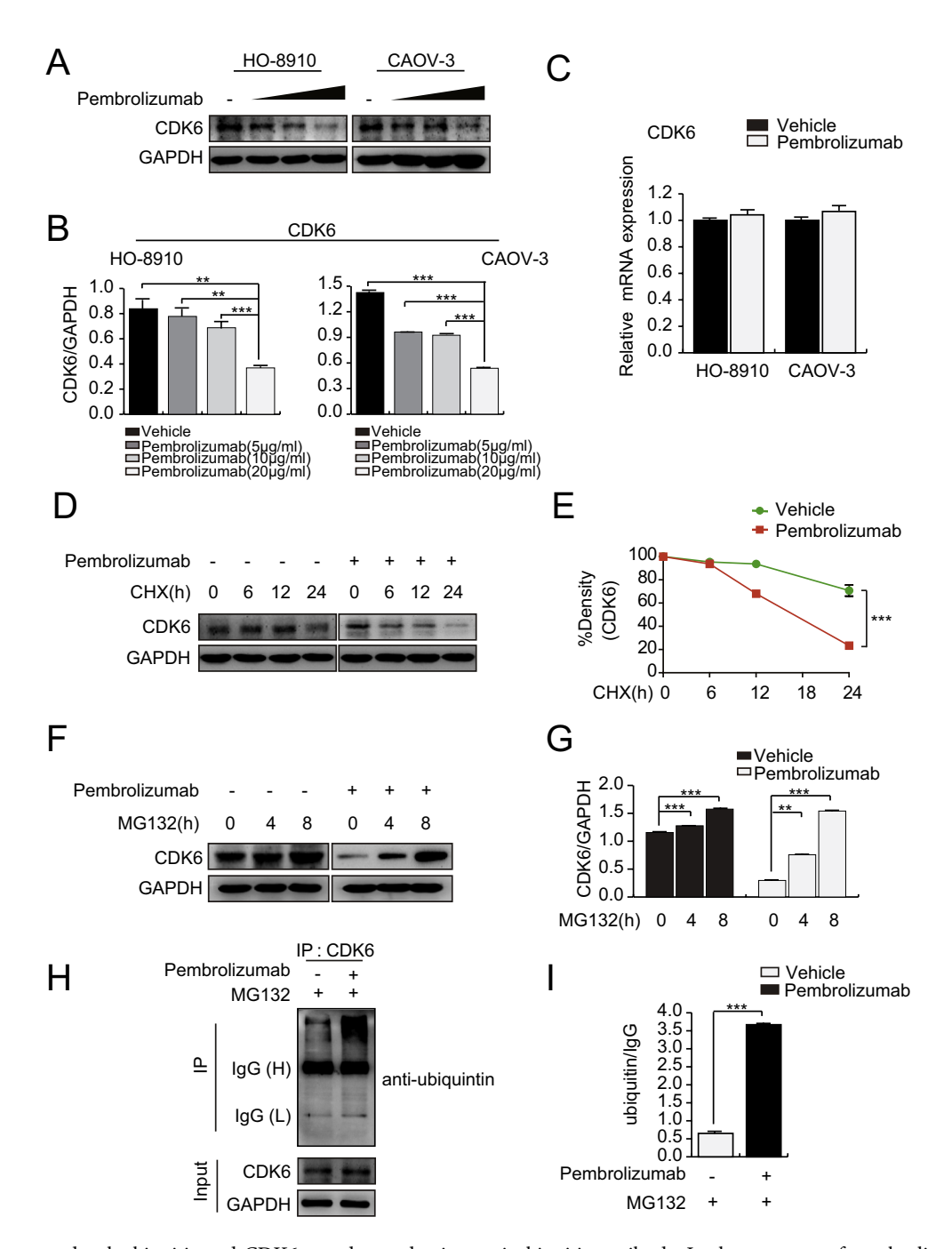


Fig. 2. Pembrolizumab blocks G0/G1 to S phase transition in ovarian cancer cells. (A) HO-8910 and CAOV-3 cells exposed to  $20 \mu g/mL$  pembrolizumab were subjected to flow cytometry analysis. (B) The percentage of cells in G0/G1 phase, S phase and G2/M phase at 48 h was shown in the graphs respectively.

in CAOV-3 cell lines were decreased significantly following pembrolizumab treatment (Fig. 3A and 3B right panel; Supplementary Fig. 3). Meanwhile, quantitative Real-time PCR experiments did not show any influence of pembrolizumab on CDK6 mRNA levels in HO-8910 and CAOV-3 cells, indicating that the treatment of pembrolizumab only caused the decrease in protein levels of CDK6, but not mRNA levels. (Fig. 3C). These findings suggested pembrolizumab-induced downregulation of CDK6 may be mediated by post-translational modifications.

To further validate whether pembrolizumab affected CDK6 expression in a proteasome-dependent manner, we treated indicated cells with the protein synthesis inhibitor cycloheximide (CHX). Notably, the half-life of CDK6 protein was prominently reduced from more than 24 h in control to less than 6 h in the pembrolizumab-treated cells, suggesting that pembrolizumab treatment accelerated CDK6 degradation (Fig. 3D and E; Supplementary Fig. 4). Subsequently, HO-8910 cells with or without pembrolizumab were treated by the proteasome inhibitor MG132 for the indicated time. Western blotting analysis of HO-8910 ovarian cancer cell lysates showed that while pembrolizumab treatment reduced levels of CDK6, MG132 treatment reversed this effect, leading to dramatic accumulation of CDK6 protein levels in a timely fashion (Fig. 3F and 3G; Supplementary Fig. 5).

Given that the ubiquitin-proteasome system plays a critical role in protein degradation, we preformed general ubiquitination assays to investigate the effect of pembrolizumab on ubiquitination of CDK6. Cells were treated with MG132 for 6 h before protein sample collection to inhibit proteasomal degradation, so that polyubiquitinated CDK6 can be accumulated and detected later. Endogenous CDK6 protein was pulled down,



and polyubiquitinated CDK6 was detected using anti-ubiquitin antibody. In the presence of pembrolizumab, higher polyubiquitination level was observed for CDK6 (Fig. 3 H and I; Supplementary Fig. 6). Collectively, these results indicated that pembrolizumab decreased the stability of CDK6 via promoting polyubiquitination of CDK6 in HO-8910 cells.

#### Pembrolizumab suppresses migratory capacity of ovarian cancer cells

To examine whether pembrolizumab exhibited an inhibitory role on the migration of OC cells, we performed wound-healing and transwell migration assays in HO-8910 and CAOV-3 cells. Wound-healing assays showed pembrolizumab treatment resulted in a remarkable reduction in migration capacity of HO-8910 and CAOV-3 cells, as presented in Fig. 4A-D. Consistent with above results, transwell migration experiments also confirmed the suppressive influence of pembrolizumab on cell mobility (Fig. 4E-G). Taken together, our results demonstrated that pembrolizumab blocked OC cell migration in vitro 14.

#### Pembrolizumab regulates the expression of EMT-related markers in ovarian cancer cells

Having shown that pembrolizumab represses cell migration in ovarian cancer, we thus turn to investigate the underlying molecular mechanisms for inhibitory activities. The above results suggested that pembrolizumab-induced polyubiquitination of CDK6 attenuate the protein stability of CDK6. It has been reported that CDK6 is involved in regulating EMT and metastasis through stabilizing Snail in breast cancer and depletion of CDK6 in

**∢Fig. 3**. Pembrolizumab decreases the stability of CDK6 protein in ovarian cancer cells. (**A-B**) HO-8910 and CAOV-3 cells were exposed to the different concentrations of pembrolizumab for 48 h. Western blotting was performed to determine the expression levels of CDK6. The blots were cut prior to hybridisation with antibodies during blotting. The data are expressed as mean ± SEM. \*\*P < 0.01; \*\*\*P < 0.001 compared with Control group (0 μg/mL pembrolizumab). (C) HO-8910 and CAOV-3 cells were exposed to 20 μg/ mL pembrolizumab for 24 h and the mRNA levels of CDK6 were detected by quantitative RT-PCR, and normalized to 18S mRNA levels. The data are expressed as mean ± SEM. (D) HO-8910 cells were pretreated with pembrolizumab (20µg/mL) for 48 h and harvested at indicated time points after treatment with CHX (80 µg/mL). The changes in the protein expressions of CDK6 was analyze by Western blotting with indicated antibody. The blots were cut prior to hybridisation with antibodies during blotting. (E) Relative CDK6 protein levels standardized by GAPDH. \*\*\*P<0.001 compared with Control group (CHX-untreated group). (F) HO-8910 cells were pretreated with pembrolizumab for 48 h, and both pembrolizumab-untreated and pembrolizumab-treated cells were harvested at indicated time points after treatment with MG132 (20 µmol/L). The change of CDK6 protein expression was detected by Western blotting with indicated antibody. The blots were cut prior to hybridisation with antibodies during blotting. (G) Graph showed relative CDK6 protein levels determined by densitometric quantification analysis and normalized by GAPDH level. The data are expressed as mean ± SEM. \*\*\*P < 0.001 compared with Control group (MG132 0 h group) respectively. (H) HO-8910 cells were treated with or without 20 µg/mL pembrolizumab for 48 h and harvested at 6 h after treatment with MG132 (20 µmol/L). Lysates were subjected to immunoprecipitation with anti-CDK6 antibody, followed by immunoblotting with anti-CDK6 and anti-ubiquitin antibodies. (I) Graph showed relative ubiquitinated-CDK6 protein levels determined by densitometric quantification analysis and normalized by IgG (H) level. The data are expressed as mean  $\pm$  SEM. \*\*\*P<0.001 compared with Control group (pembrolizumab-untreated group).

breast cancer cells decreased the protein expression of Snail<sup>15</sup>. Thus, we detected the effect of pembrolizumab on Snail expression in OC cells. As shown in Fig. 5A -C, the protein levels of Snail decreased in a dose-dependent manner by pembrolizumab treatment for 48 h in HO-8910 and CAOV-3 cells. Accumulating experimental and clinical evidences demonstrated that Snail promotes EMT<sup>15</sup>. We thus turn to explore whether downregulation of Snail by pembrolizumab inhibits EMT. The results demonstrated that a concentration-dependent increase in the level of an epithelial marker E-cadherin, while the expression of mesenchymal markers N-cadherin and Vimentin decreased after pembrolizumab treatment in both HO-8910 and CAOV-3 cell lines. (Fig. 5A-C; Supplementary Fig. 7; Supplementary Fig. 8). Collectively, specific molecular changes associated with EMT indicated pembrolizumab repressed EMT, resulting in loss of migratory capacity.

## Pembrolizumab enhances effect of cisplatin on suppressing cancer cell proliferation in ovarian cancer cells

Previous studied have reported that CDK6 silencing sensitizes ovarian cancer cells to platinum  $^{14}$ . Having established that pembrolizumab treatment leads to instability of CDK6 and increases degradation speed of CDK6, we therefore evaluated whether the combination of pembrolizumab and cisplatin enhances antiproliferative effects of cisplatin on OC cell line HO-8910. HO-8910 cells were treated with vehicle, pembrolizumab (10  $\mu$ g/mL), cisplatin (10  $\mu$ g/mL) or cisplatin (10  $\mu$ g/mL) combined with pembrolizumab (10  $\mu$ g/mL), respectively, for 48 h and then CCK-8 assays were performed to detect cell viability. As shown in Fig. 6, IC50 of HO-8910 to pembrolizumab and cisplatin was 9.643  $\mu$ g/mL in combined treatment. Co-treatment with cisplatin and pembrolizumab showed a significantly greater inhibitory effect on HO-8910 cell viability than treatment with pembrolizumab alone, cisplatin alone or vehicle, suggesting pembrolizumab enhances cisplatin-induced repression of proliferation in HO-8910 cells.

#### Discussion

Activation of PD-1/PD-L1 signaling serves as a principal mechanism by which tumors evade antigen-specific T-cell immunologic responses<sup>7</sup>. Otherwise, antibodies blocking PD-1 or PD-L1 reverse this process, augment T-cell function in the tumor microenvironment and enhance antitumor immune activity<sup>7</sup>. Pembrolizumab is a humanized monoclonal antibody targeting programmed cell death protein 1 (PD-1) found on T and pro-B cells<sup>8</sup>. Pembrolizumab prevents PD-1 ligation by both PD-L1 and PD-L2, preventing the immune dysregulation that otherwise occurs when T-cells encounter cells expressing these ligands8. Currently, pembrolizumab is tested in 12 categories of malignancies including ovarian cancer to determine its clinical efficacy<sup>16,17</sup>. In addition, resent researches demonstrated that the functional role of PD-1 is currently being extended into nonimmune cell types<sup>18-21</sup>. Tumor cell-intrinsic PD-1 promotes tumorigenesis in melanoma, hepatocellular carcinoma, pancreatic ductal adenocarcinoma, thyroid cancer, glioblastoma, and triple-negative breast cancer independently of adaptive immunity<sup>22-27</sup>. PD-1 targeted antibody treatment reduces the cell growth of ovarian and bladder cancer cells in the absence of adaptive immunity<sup>18</sup>. Therefore, we wondered that whether pembrolizumab has direct anti-tumor effect on ovarian cancer cells. In the present study, we detected the action of pembrolizumab in ovarian cancer cell lines, including HO-8910 cells and CAOV-3 cells. Our study showed that pembrolizumab treatment markedly suppressed the proliferation, cell cycle progression and migration in both HO-8910 and CAOV-3 cells. In addition, CCK-8 assays showed that the treatment of pembrolizumab (20 µg/mL) for 24 h didn't inhibit the proliferation of HO-8910 and CAOV-3 cells until treatment for 48 h, suggesting prolonged treatment of pembrolizumab exhibits direct anti-proliferative activity in OC cells.

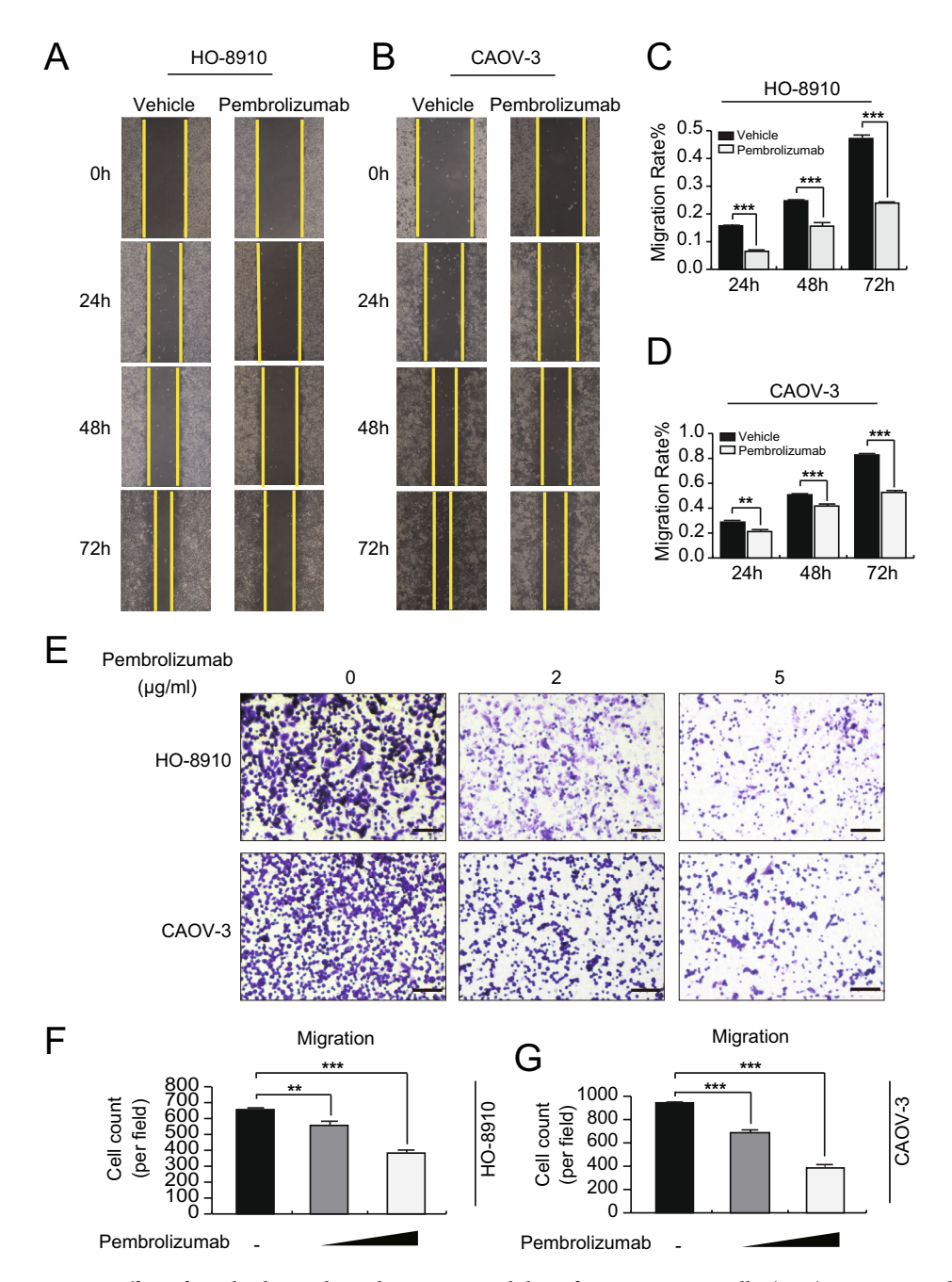


Fig. 4. Effect of pembrolizumab on the migration ability of ovarian cancer cells. (A-B) HO-8910 and CAOV-3 cells were treated with or without pembrolizumab and subjected to wound-healing assays. Representative images were shown. (C-D) The statistical analysis of wound-healing assay by Image J. The data are expressed as mean  $\pm$  SEM. \*\*P<0.01; \*\*\*P<0.001 compared with Control group (Vehicle group). (E) HO-8910 and CAOV-3 cells were treated with the indicated concentrations of pembrolizumab for 15 h and subjected to Transwell migration assays. Representative images were shown. Scar bar: 100  $\mu$ m. (F-G) The statistical analysis of Transwell migration assays by Image J. The data are expressed as mean  $\pm$  SEM. \*\*P<0.01; \*\*\*P<0.001 compared with Control group (pembrolizumab-untreated group).

Cell proliferation is supposed to primarily regulate in the G1 phase of cell cycle, and the abnormal regulation of the transition from G1 to S phase can cause neoplastic transformation<sup>28–31</sup>. Cyclin-dependent kinase 6 (CDK6) is a major factor that contributes to cellular transition from the G1 phase of the cell cycle to the S phase by forming a complex combined with CyclinD1 and CDK4<sup>32</sup>. Compared with normal cells, CDK6 expression is generally up-regulated in cancer cells and its enforced expression is closely associated with progression of several types of cancers<sup>32</sup>. Recent studies show that SUMO1 modification stabilizes CDK6 protein and drives the cell cycle and glioblastoma progression<sup>33</sup>. As well, inhibition of ubiquitin-conjugating enzyme 2 N (UBE2N)-dependent CDK6 protein degradation by miR-934 promotes human bladder cancer cell growth<sup>32</sup>. These findings suggest CDK6 plays an important role in cancer cell growth and proliferation and represents a promising target for

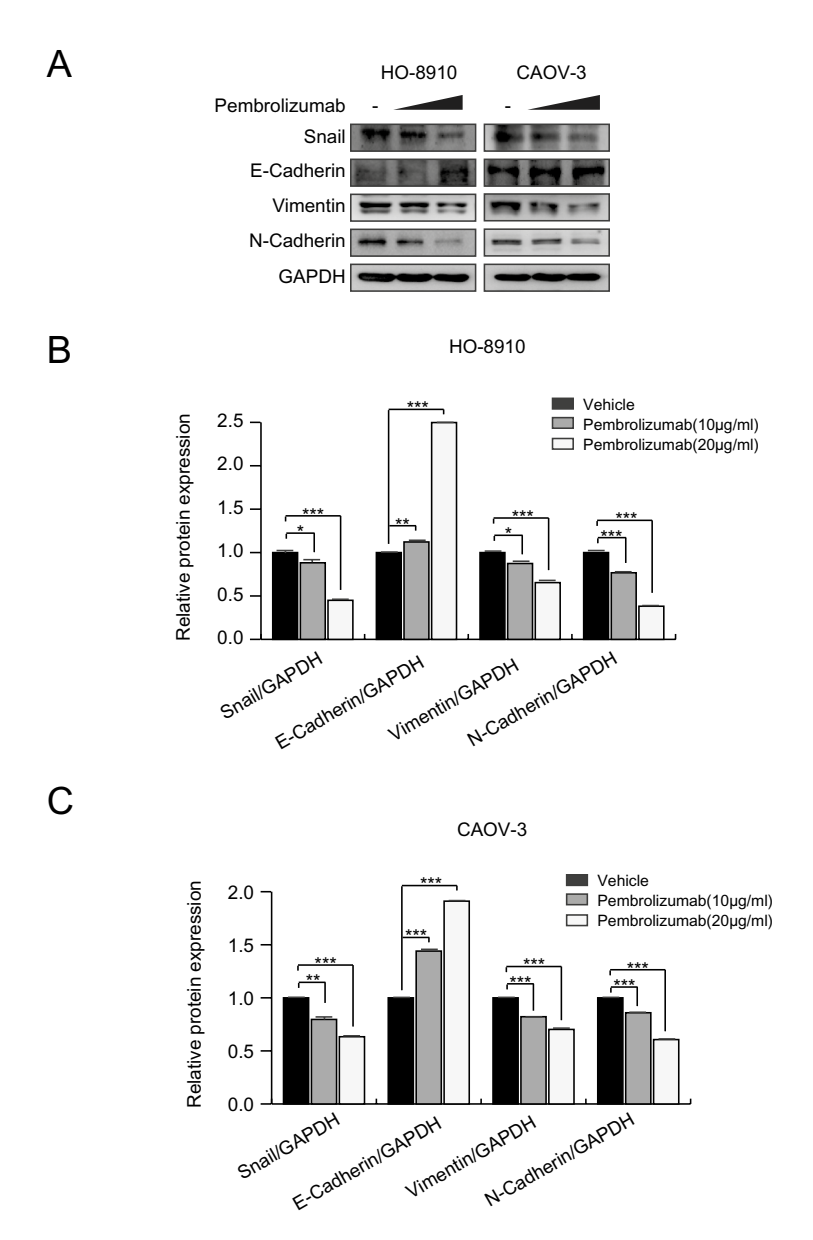


Fig. 5. Effect of pembrolizumab on the expression of EMT related makers in ovarian cancer cells. (A) HO-8910 and CAOV-3 cells were exposed to the different concentrations of pembrolizumab for 48 h. Western blotting assays were performed to evaluate the protein levels of snail, E-cadherin, Vimentin and N-cadherin. The blots were cut prior to hybridisation with antibodies during blotting. (B-C) Graph showed relative snail, E-cadherin, Vimentin and N-cadherin protein levels determined by densitometric quantification analysis and normalized by GAPDH level. The data are represented as mean  $\pm$  SEM. \*P<0.05; \*\*P<0.01; \*\*\*P<0.001 compared with Control group (pembrolizumab-untreated group).

anti-cancer therapy. In addition, the CDK4/6 pathway intersects with several key mitogenic signaling pathways in cancer cells, such as PI3K-AKT-mTOR pathways and RAS-RAF-MEK-ERK signaling pathway<sup>34</sup>. It has been reported that CDK4/6 inhibitors may trigger antitumor immunity in solid tumors<sup>34–39</sup> and in vivo experiments verified synergistic effects of CDK4/6 inhibition with programmed cell death 1 (PD-1) blockade, which lead to elevated tumor regression and better overall survival rates<sup>34,39,40</sup>, implying that there are inherent connections between the PD-1 pathway and the CDK4/6 pathway. Furthermore, flow cytometry analysis in our study showed that pembrizumab (PD-1 inhibitor) significantly delayed cell G1-S phase transition. Thus, we hypothesized that the PD-1 and CDK4/6 pathways can interact and pembrizumab treatment may weaken the expression or activity of CDK4/6. Herein, we demonstrated that treatment with pembrolizumab markedly decreased the protein expression of CDK6, but not CDK4. The change in CDK6 then led to a block in G1/S progression and suppression of cell growth and proliferation of OC cells. Taken together, our data hinted pembrolizumab may inhibit cell proliferative ability in OC, by targeting CDK6.

In tumor cells, CDK6 is frequently upregulated and CDK4/6 kinase inhibitors like palbociclib possess high activity in breast cancer and other malignancies<sup>10</sup>. Besides its crucial catalytic function, kinase-independent

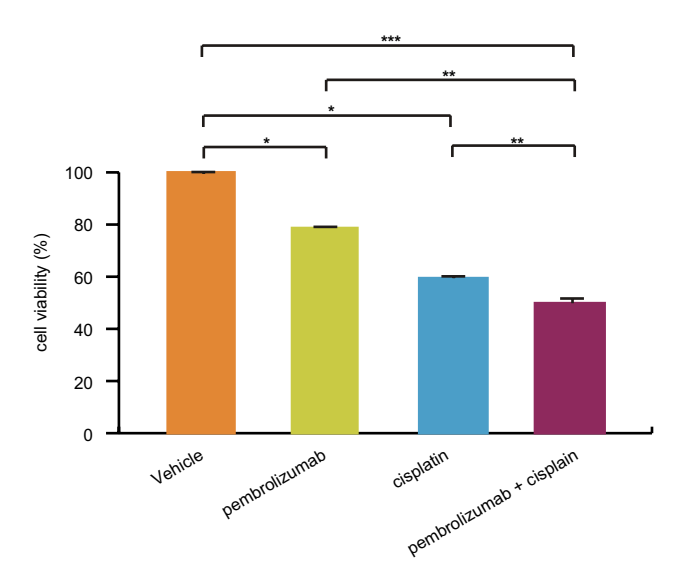


Fig. 6. Effects of combination of pembrolizumab and cisplatin on HO8910 cell proliferation. (A) HO-8910 cells were exposed to vehicle, pembrolizumab (10  $\mu$ g/mL), cisplatin (10  $\mu$ g/mL) or cisplatin (10  $\mu$ g/mL) combined pembrolizumab (10  $\mu$ g/mL) for 48 h. And then CCK-8 assays were performed to determine cell viability. Statistical analysis was carried out between cells treated with vehicle and each of the other drug groups, and pembrolizumab or cisplatin alone group and combination of cisplatin and pembrolizumab group. The data are expressed as mean  $\pm$  SEM. \*P<0.05; \*P<0.001; \*\*P<0.001.

roles of CDK6 have been described. For instance, CDK6, as transcriptional regulator, regulates and induces important proto-oncogenes including vascular endothelial growth factor A (VEGFA), fms-related tyrosine kinase 3 (FLT3), aurora kinase (AURK) and AKT, that are crucial for survival, proliferation and angiogenesis in acute lymphoblastic leukemia and acute myeloid leukemia<sup>35,41-44</sup>. Therefore, targeted degradation of CDK6 may be advantageous over kinase inhibition<sup>10</sup>. It has been indicated that CDK6 protein degradation is mediated by ubiquitin-related pathways<sup>32</sup>. Our results demonstrated that upon inhibition of protein synthesis by cycloheximide, pembrolizumab-treated cells showed a faster rate of CDK6 degradation compared to control cells. Meanwhile, proteasome inhibition by MG132 resulted in the significant accumulation of CDK6, confirming that the pembrolizumab-induced degradation of CDK6 was mediated by CDK6 polyubiquitination and proteasomal degradation, implying pembrolizumab may serve as potential pharmacologic CDK6-targeting degraders. However, further studies will be required to better understand the mechanism by which pembrolizumab is involved in facilitating CDK6 polyubiquitination and degradation in OC cells.

Epithelial-to-mesenchymal transition (EMT) is a highly conserved process in which polarized, immotile epithelial cells lose adherent and tight junctions, and become migratory mesenchymal cells<sup>45</sup>. Snail is a prominent inducer of EMT and strongly represses E-cadherin expression<sup>45,46</sup>. A previous study has reported that knockdown of CDK6 in breast cancer cells decreases Snail protein expression. Moreover, we have already reported that pembrolizumab induced reduction of CDK6 protein expression in a dose-dependent manner. Based on these facts, we speculated that pembrolizumab treatment might decrease the expression of Snail, which promotes EMT. Western blotting analyses demonstrated the levels of Snail, Vimentin and N-cadherin were significantly reduced upon pembrolizumab treatment, but E-cadherin was increased. In addition, we showed that the migration of OC cells was strongly inhibited by pembrolizumab, as shown by the wound healing and the transwell assay. Thus, these findings suggested that has suppressive effect of pembrolizumab on cell movement and cell migration in OC cells may be related to downregulation of EMT marker proteins.

Emerging evidence suggests that CDK6 represents an actionable target that can be exploited to improve platinum efficacy in epithelial ovarian cancer (ECO) patients<sup>14</sup>. Studies have shown that silencing or pharmacological inhibition of CDK6 increases EOC cell sensitivity to platinum<sup>14</sup>. Data presented here demonstrated that pembrolizumab induced destabilization of CDK6 through polyubiquitin-mediated proteasomal degradation. We therefore investigated whether pembrolizumab affected anti-cancer activity of cisplatin. Our results indicated that a combination of pembrolizumab and cisplatin resulted in increased inhibition of cell proliferation in HO-8910 cells, implying that pembrolizumab may serve as a promising candidate drug for cisplatin-resistant patients of OC.

In conclusion, our studies provided a novel mechanism of regulation of CDK6 expression by pembrolizumab through the ubiquitin–proteasome system in OC cells. Pembrolizumab suppressed CDK6-related cell proliferation, migration and cell cycle progression in OC cells in vitro. Therefore, the present study sheds light on the mechanism of direct anti-cancer activity of pembrolizumab and broadens clinical application prospects of pembrolizumab for the treatment of ovarian cancer.

#### Data availability

The data that support the findings of this study are available from the corresponding author upon reasonable request.

Received: 18 December 2024; Accepted: 8 July 2025

Published online: 12 July 2025

#### References

- 1. Bray, F. et al. Global cancer statistics 2022: GLOBOCAN estimates of incidence and mortality worldwide for 36 cancers in 185 countries. CA: A Cancer Journal for Clinicians 74, 229-263, https://doi.org/10.3322/caac.21834 (2024).
- 2. Zhang, Q. F. et al. CDK4/6 inhibition promotes immune infiltration in ovarian cancer and synergizes with PD-1 blockade in a B cell-dependent manner. Theranostics 10, 10619–10633. https://doi.org/10.7150/thno.44871 (2020).
- 3. Jacobs, I. J. et al. Ovarian cancer screening and mortality in the UK collaborative trial of ovarian cancer screening (UKCTOCS): A randomised controlled trial. Lancet 387, 945-956. https://doi.org/10.1016/S0140-6736(15)01224-6 (2016)
- 4. Karam, A. et al. Fifth ovarian cancer consensus conference of the gynecologic cancer intergroup: First-line interventions. Ann. Oncol. 28, 711-717. https://doi.org/10.1093/annonc/mdx011 (2017).
- 5. Luvero, D., Milani, A. & Ledermann, J. A. Treatment options in recurrent ovarian cancer: latest evidence and clinical potential. Ther. Adv. Med. Oncol. 6, 229-239. https://doi.org/10.1177/1758834014544121 (2014).
- 6. Ai, L. et al. Research Status and Outlook of PD-1/PD-L1 Inhibitors for Cancer Therapy. Drug. Des. Devel. Ther. 14, 3625-3649. https://doi.org/10.2147/DDDT.S267433 (2020).
- 7. Palumbo, G. et al. Pembrolizumab in lung cancer: current evidence and future perspectives. Future Oncol. 15, 3327-3336. https:// doi.org/10.2217/fon-2019-0073 (2019).
- 8. England, C. G. et al. Preclinical Pharmacokinetics and Biodistribution Studies of 89Zr-Labeled Pembrolizumab. J. Nucl. Med 58, 162-168. https://doi.org/10.2967/jnumed.116.177857 (2017).
- 9. Matulonis, U. A. et al. Antitumor activity and safety of pembrolizumab in patients with advanced recurrent ovarian cancer: results from the phase II KEYNOTE-100 study. Ann. Oncol. 30, 1080-1087. https://doi.org/10.1093/annonc/mdz135 (2019).
- Steinebach, C. et al. Systematic exploration of different E3 ubiquitin ligases: an approach towards potent and selective CDK6 degraders. Chem. Sci. 11, 3474-3486. https://doi.org/10.1039/d0sc00167h (2020).
- 11. Tadesse, S., Yu, M., Kumarasiri, M., Le, B. T. & Wang, S. Targeting CDK6 in cancer: State of the art and new insights. Cell Cycle 14, 3220-3230. https://doi.org/10.1080/15384101.2015.1084445 (2015).
- 12. Su, S. et al. Potent and preferential degradation of CDK6 via proteolysis targeting chimera degraders. J. Med. Chem. 62, 7575-7582.
- https://doi.org/10.1021/acs.jmedchem.9b00871 (2019). 13. Duan, L. et al. MuiR-182-5p functions as a tumor suppressor to sensitize human ovarian cancer cells to cisplatin through direct
- targeting the cyclin dependent kinase 6 (CDK6). J BUON 25, 2279-2286 (2020). 14. Dall'Acqua, A. et al. CDK6 protects epithelial ovarian cancer from platinum-induced death via FOXO3 regulation. EMBO Mol.
- Med. 9, 1415-1433. https://doi.org/10.15252/emmm.201607012 (2017). Liu, T. et al. CDK4/6-dependent activation of DUB3 regulates cancer metastasis through SNAIL1. Nat. Commun. 8, 13923. https:/
- /doi.org/10.1038/ncomms13923 (2017). 16. Kwok, G., Yau, T. C., Chiu, J. W., Tse, E. & Kwong, Y. L. Pembrolizumab (Keytruda). Hum. Vaccin. Immunother. 12, 2777–2789.
- https://doi.org/10.1080/21645515.2016.1199310 (2016). 17. Andrikopoulou, A. et al. Pembrolizumab in combination with bevacizumab and oral cyclophosphamide in heavily pre-treated
- platinum-resistant ovarian cancer. Int. J. Gynecol. Cancer 33, 571-576. https://doi.org/10.1136/ijgc-2022-003941 (2023 Wang, X. et al. Tumor cell-intrinsic PD-1 receptor is a tumor suppressor and mediates resistance to PD-1 blockade therapy. Proc. Natl. Acad. Sci. U S A 117, 6640-6650. https://doi.org/10.1073/pnas.1921445117 (2020).
- 19. Yao, H., Wang, H., Li, C., Fang, J. Y. & Xu, J. Cancer Cell-Intrinsic PD-1 and Implications in Combinatorial Immunotherapy. Front. Immunol. 9, 1774. https://doi.org/10.3389/fimmu.2018.01774 (2018).
- 20. Zheng, H. et al. New insights into the important roles of tumor cell-intrinsic PD-1. Int. J. Biol. Sci. 17, 2537-2547. https://doi.org/ 10.7150/ijbs.60114 (2021).
- 21. Chen, M., Bie, L. & Ying, J. Cancer cell-intrinsic PD-1: Its role in malignant progression and immunotherapy. Biomed. Pharmacother. https://doi.org/10.1016/j.biopha.2023.115514 (2023).
- 22. Kleffel, S. et al. Melanoma cell-intrinsic PD-1 receptor functions promote tumor growth. Cell 162, 1242-1256. https://doi.org/10. 1016/j.cell.2015.08.052 (2015).
- 23. Li, H. et al. Programmed cell death-1 (PD-1) checkpoint blockade in combination with a mammalian target of rapamycin inhibitor restrains hepatocellular carcinoma growth induced by hepatoma cell-intrinsic PD-1. Hepatology 66, 1920-1933. https://doi.org/10. 1002/hep.29360 (2017)
- 24. Pu, N. et al. Cell-intrinsic PD-1 promotes proliferation in pancreatic cancer by targeting CYR61/CTGF via the hippo pathway. Cancer Lett. 460, 42-53. https://doi.org/10.1016/j.canlet.2019.06.013 (2019).
- Liotti, F. et al. PD-1 blockade delays tumor growth by inhibiting an intrinsic SHP2/Ras/MAPK signalling in thyroid cancer cells. J. Exp. Clin. Cancer Res. 40, 22. https://doi.org/10.1186/s13046-020-01818-1 (2021).
- 26. Mirzaei, R. et al. PD-1 independent of PD-L1 ligation promotes glioblastoma growth through the NFkappaB pathway. Sci Adv 7, eabh2148. https://doi.org/10.1126/sciadv.abh2148 (2021).
- 27. Wu, Q. et al. YB-1 promotes cell proliferation and metastasis by targeting cell-intrinsic PD-1/PD-L1 pathway in breast cancer. Int. J. Biochem. Cell. Biol. 153, 106314. https://doi.org/10.1016/j.biocel.2022.106314 (2022).
- Hosokawa, Y., Onga, T. & Nakashima, K. Induction of D2 and D3 cyclin-encoding genes during promotion of the G1/S transition by prolactin in rat Nb2 cells. Gene 147, 249-252. https://doi.org/10.1016/0378-1119(94)90075-2 (1994).
- 29. Cole, A. M. et al. Cyclin D2-cyclin-dependent kinase 4/6 is required for efficient proliferation and tumorigenesis following Apc loss. Cancer Res. 70, 8149-8158. https://doi.org/10.1158/0008-5472.CAN-10-0315 (2010).
- 30. Doerner, P., Jorgensen, J. E., You, R., Steppuhn, J. & Lamb, C. Control of root growth and development by cyclin expression. Nature 380, 520-523. https://doi.org/10.1038/380520a0 (1996).
- 31. Wang, X. et al. BAP18 is involved in upregulation of CCND1/2 transcription to promote cell growth in oral squamous cell carcinoma. EBioMedicine 53, 102685. https://doi.org/10.1016/j.ebiom.2020.102685 (2020).
- $32. \ Yan, H.\ et\ al.\ Inhibition\ of\ UBE2N-dependent\ CDK6\ protein\ degradation\ by\ miR-934\ promotes\ human\ bladder\ cancer\ cell\ growth.$ FASEB J. 33, 12112-12123. https://doi.org/10.1096/fj.201900499RR (2019) 33. Bellail, A. C., Olson, J. J. & Hao, C. SUMO1 modification stabilizes CDK6 protein and drives the cell cycle and glioblastoma
- progression. Nat. Commun. 5, 4234. https://doi.org/10.1038/ncomms5234 (2014). Goel, S., DeCristo, M. J., McAllister, S. S. & Zhao, J. J. CDK4/6 inhibition in Cancer: beyond cell cycle arrest. Trends Cell. Biol. 28,
- 911-925. https://doi.org/10.1016/j.tcb.2018.07.002 (2018). Nebenfuehr, S., Kollmann, K. & Sexl, V. The role of CDK6 in cancer. Int. J. Cancer 147, 2988-2995. https://doi.org/10.1002/ijc.330
- 54 (2020).

- 36. Teo, Z. L. et al. Combined CDK4/6 and PI3Kalpha Inhibition Is Synergistic and Immunogenic in Triple-Negative Breast Cancer. Cancer Res. 77, 6340–6352. https://doi.org/10.1158/0008-5472.CAN-17-2210 (2017).
- 37. Goel, S. et al. CDK4/6 inhibition triggers anti-tumour immunity. Nature 548, 471–475. https://doi.org/10.1038/nature23465 (2017).
- 38. Schaer, D. A. et al. The CDK4/6 Inhibitor abemaciclib induces a t cell inflamed tumor microenvironment and enhances the efficacy of PD-L1 checkpoint blockade. Cell. Rep. 22, 2978–2994. https://doi.org/10.1016/j.celrep.2018.02.053 (2018).
- 39. Deng, J. et al. CDK4/6 Inhibition Augments Antitumor Immunity by Enhancing T-cell Activation. Cancer Discov. 8, 216–233. https://doi.org/10.1158/2159-8290.CD-17-0915 (2018).
- 40. Zhang, J. et al. Cyclin D-CDK4 kinase destabilizes PD-L1 via cullin 3-SPOP to control cancer immune surveillance. *Nature* 553, 91–95. https://doi.org/10.1038/nature25015 (2018).
- Kollmann, K. et al. A kinase-independent function of CDK6 links the cell cycle to tumor angiogenesis. Cancer Cell 24, 167–181. https://doi.org/10.1016/j.ccr.2013.07.012 (2013).
- 42. Uras, I. Z. et al. Palbociclib treatment of FLT3-ITD+ AML cells uncovers a kinase-dependent transcriptional regulation of FLT3 and PIM1 by CDK6. Blood 127, 2890–2902. https://doi.org/10.1182/blood-2015-11-683581 (2016).
- Hydbring, P., Malumbres, M. & Sicinski, P. Non-canonical functions of cell cycle cyclins and cyclin-dependent kinases. Nat. Rev. Mol. Cell. Biol. 17, 280–292. https://doi.org/10.1038/nrm.2016.27 (2016).
- 44. Uras, I. Z. et al. Therapeutic Vulnerabilities in FLT3-Mutant AML Unmasked by Palbociclib. *Int. J. Mol. Sci.* https://doi.org/10.339 0/ijms19123987 (2018).
- 45. Wang, Y., Shi, J., Chai, K., Ying, X. & Zhou, B. P. The role of snail in EMT and tumorigenesis. Curr. Cancer Drug. Targets 13, 963-972. https://doi.org/10.2174/15680096113136660102 (2013).
- 46. Barrallo-Gimeno, A. & Nieto, M. A. The Snail genes as inducers of cell movement and survival: implications in development and cancer. *Development* 132, 3151–3161. https://doi.org/10.1242/dev.01907 (2005).

#### **Author contributions**

Yi Wu designed this program and wrote the manuscript. Ziyan Xu conducted the cell experiments. Zuqiang Kou completed the data collection and analysis. Qiuling Ye, Liting Chen and Boyu Gou performed molecular biology experiments. All authors read and approved the final manuscript.

#### **Funding**

This study was supported by Natural Science Foundation of Liaoning Province (2022-MS-412) and College Student Project of Shenyang Medical College (20239043).

#### **Declarations**

#### Competing interests

The authors declare no competing interests.

#### Additional information

**Supplementary Information** The online version contains supplementary material available at https://doi.org/1 0.1038/s41598-025-11043-5.

Correspondence and requests for materials should be addressed to Y.W.

Reprints and permissions information is available at www.nature.com/reprints.

**Publisher's note** Springer Nature remains neutral with regard to jurisdictional claims in published maps and institutional affiliations.

**Open Access** This article is licensed under a Creative Commons Attribution-NonCommercial-NoDerivatives 4.0 International License, which permits any non-commercial use, sharing, distribution and reproduction in any medium or format, as long as you give appropriate credit to the original author(s) and the source, provide a link to the Creative Commons licence, and indicate if you modified the licensed material. You do not have permission under this licence to share adapted material derived from this article or parts of it. The images or other third party material in this article are included in the article's Creative Commons licence, unless indicated otherwise in a credit line to the material. If material is not included in the article's Creative Commons licence and your intended use is not permitted by statutory regulation or exceeds the permitted use, you will need to obtain permission directly from the copyright holder. To view a copy of this licence, visit <a href="http://creativecommons.org/licenses/by-nc-nd/4.0/">http://creativecommons.org/licenses/by-nc-nd/4.0/</a>.

© The Author(s) 2025